Supporting information for

Anaerobic Photocatalytic Dihydroxylation of Propylene to Propylene Glycol and Hydrogen at Ambient Temperature and Pressure

Xinyu Song[a], Wei Wang[a], Xiaomin Lao[a], Yitong Liu[a], Huanmin Liu[a], Peng Zhou[a, b, c*]

[a]School of Environment and Energy, Peking University Shenzhen Graduate School, Shenzhen 518055, PR China

[b]Eco-environment and Resource Efficiency Research Laboratory, School of Environment and Energy, Peking University Shenzhen Graduate School, Shenzhen 518055, PR China

[c]Guangdong Provincial Key Lab of Nano-Micro Material Research, Peking University Shenzhen Graduate School, Guangdong 518055, PR China

*Corresponding author.

Email address: pengzhou1209@pku.edu.cn

1 Characterization methods

Text 1. DFT Computational Details

The photocatalytic conversion of C_3H_6 to 1,2-PG over M-TiO_2 catalysts (M = Ag, Au, Pd, Pt, Ru, Rh) was systematically investigated using density functional theory (DFT) calculations as implemented in the VASP package. The revised Perdew−Burke−Ernzerhof (RPBE) functional was adopted to treat exchange-correlation interactions. Electron-core interactions were described using the projector augmented-wave (PAW) pseudopotential. The TiO_2[1] surface, modeled as a 4 × 2 supercell with four trilayer O–Ti–O stacks, served as the substrate for all metal modifications. Structural optimizations were carried out with an energy cutoff of 450 eV at the Gamma point until atomic forces converged below 0.001 eV $Å^{-1}$. Subsequently, the projected density of states (PDOS) was computed using a 2 × 4 × 1 Monkhorst−Pack k-point mesh and the same energy cutoff. The Gibbs free energy change (ΔG) for each elementary step was computed within the standard hydrogen electrode (SHE) model via the relation:

$$G=E+ZPE-TS$$

where E represents the electronic energy from DFT, ZPE the zero-point energy, and S the entropy at 298.15 K, respectively.

Text 2. Chemical Reagents

P25 titanium dioxide (P25, TiO_2), chloroplatinic acid hydrate ($H_2PtCl_6 \cdot xH_2O$, ≥ 99.9%), potassium tetrachloropalladate (K_2PdCl_4, ≥ 99.9%), deuterium oxide (D_2O), 2,2,6,6-tetramethylpiperidine-1-oxyl (TEMPO), and propylene oxide (C_3H_6O, ≥ 99.5%) were purchased from Aladdin (Shanghai, China). Silver nitrate ($AgNO_3$), ruthenium(III) chloride anhydrous ($RuCl_3$, 99.99%), rhodium trichloride ($RhCl_3$, 99.0%), gold(III) chloride ($AuCl_3$, 98.0%), methanol (CH_3OH, ≥ 99.9%), acetaldehyde (C_2H_4O, 99.5%), *n*-propanal (C_3H_6O, 97.0%), isopropyl alcohol (C_3H_8O, ≥ 99.5%), *n*-propanol (C_3H_8O, ≥ 99.5%), 1,2-propanediol ($C_3H_8O_2$, 99%) were purchased from Shanghai Macklin reagent company. Acryl alcohol (C_3H_6O, 100 μg mL^{-1}) was purchased from Beijing Kezhan Biotechnology Co. The FTO glass (1.0 cm × 1.8 cm) was from Heptachroma company. In the experiment, all chemical reagents were of analytical grade and used directly without further purification. Deionized water was used throughout the experiment.

Text 3. Synthesis of Catalytic Materials

Ag-TiO_2: 0.5 g of TiO_2 powder was dispersed in 30 mL of deionized water, followed by ultrasonication for 30 min to ensure complete dispersion. Then, $AgNO_3$ solution was added to the suspension, and the Ag loading was controlled to 0.1 wt%, 0.2 wt%, 0.3 wt%, 0.4 wt%, 0.5 wt%, respectively. The mixture was irradiated for photoreduction using a 300 W Xe lamp (PerfectLight Technology, PLS-SXE300E) under an oxygen atmosphere for 30 min. After the reaction, the suspension was centrifuged at 6000 r min^{-1} for 5 min to collect

the solid product. The obtained solid was vacuum-dried at 60 °C for 12 h. Subsequently, the Ag-TiO_2 photocatalyst was obtained by grinding the dried sample using an agate mortar. Ru-TiO_2, Rh-TiO_2, Pd-TiO_2, Pt-TiO_2, and Au-TiO_2 catalysts were synthesized by replacing the $AgNO_3$ with $RuCl_3$, $RhCl_3$, K_2PdCl_4, H_2PtCl_6, $AuCl_3$, $CoCl_2$, $CuCl_2$, and $NiCl_2$, respectively, while maintaining the same experimental procedures and a metal loading of 0.3 wt% for all catalysts.

Text 4. Analytical Methods

The morphology of Ag-TiO_2 was investigated using transmission electron microscope (TEM, JEM-3200FS, JEOL) and the corresponding energy-dispersive X-ray spectroscopy (EDX) mapping images were recorded on a JEOL JED-2300. Aberration-corrected high angle annular dark-field scanning transmission electron microscopy (AC-HAADF-STEM) analysis was performed on a Themis Z transmission electron microscope (accelerating voltage, 300 kV). *In-situ* X-ray photoelectron spectroscopy (XPS) measurements were performed on the Thermo Scientific ESCALAB 250Xi spectrometer (USA) using an Al Kα X-ray source with a pass energy of 200.0 eV. The optical properties were characterized by ultraviolet-visible-near-infrared diffuse reflectance spectroscopy (UV-Vis-NIR DRS) using a Agilent Cary 5000 spectrometer equipped with a diffuse reflectance accessory (integrating sphere). The spectra were collected in the range of 200–800 nm using $BaSO_4$ as the 100% reflectance reference. Electron paramagnetic resonance (EPR) spectra are recorded on a CIQTEK EPR200-Plus spectrometer (Hefei, China) at room temperature.

Text 5. Triphase Photocatalytic Oxidation of C_3H_6 to 1,2-PG

The photocatalytic propylene conversion was performed under irradiation of a 300 W Xe lamp (China Education Au-light, CEL-PF-T6). The experiment was tested using a homemade photocatalytic reactor. The reaction system, with a total volume of 290 mL, comprised two main components: (i) a photocatalytic reaction chamber featuring a cylindrical reactor (5 cm in diameter and 5 cm in height) with an illuminated surface area, and (ii) a temperature control unit equipped with an external cooling water circulation system to maintain the reaction temperature at 25 °C. A peristaltic pump was employed to ensure efficient gas circulation throughout the system. For each experiment, 10 mg of catalyst was dispersed in 20 mL of ultrapure water in the reactor. The system was then purged with C_3H_6 gas at a flow rate of 200 mL min^{-1} to completely eliminate residual oxygen. After 3 h of illumination, the liquid products and the gas products were analysed separately. Throughout the duration of the photocatalytic reaction, 0.2 mL of the gas products (H_2) was collected and subsequently injected into gas chromatography (GC2018, Shimazu, equipped with a TCD detector and 5 Å molecular sieve column, utilizing N_2 as the carrier gas). The liquid products were detected by FULI DISTRUMENT GC9090II gas chromatograph utilizing Ar as the carrier gas with FID detector. The gas products (CO_2, CH_4, C_2H_4, C_2H_6, C_3H_8 and so on) were analysed by SHIMADZU GC-2014 gas

chromatograph equipped with FID and TCD detector utilizing Ar and He as the carrier gas. All experiments were repeated two or three times, all points in the figures were the average of the results and the error bars represent the standard deviation of the average. The carbon selectivities of 1,2-PG were calculated based on the carbon numbers of all carbonaceous products:

$$\text{Selectivity (\%)}=\frac{3n(\text{1,2-PG})}{2n(\text{allyl alcohol})+3\sum n(\text{all other three-carbon products})+3n(\text{1,2-PG})+n(CO_2)}\times 100\%$$

Text 6. Electrochemical Measurements

Electrochemical measurements, including transient photocurrent response and electrochemical impedance spectroscopy (EIS), were performed using a standard three-electrode configuration on a CHI 760E electrochemical workstation. The working electrode was prepared by drop-casting the catalyst suspension onto a pre-cleaned fluorine-doped tin oxide (FTO) glass substrate (1.0 × 1.0 cm^2). Typically, 10 mg of catalyst powder was dispersed in a mixed solvent containing 1 mL deionized water, followed by ultrasonication for 30 min to obtain a uniform ink. Approximately 200 μL of this suspension was drop-cast onto the FTO surface and dried at 50 °C. A platinum foil and an Ag/AgCl (saturated KCl) electrode were used as the counter and reference electrodes, respectively. The electrolyte was 0.1 M Na_2SO_4 aqueous solution (pH 7).

EIS was conducted in the frequency range of 100 kHz to 0.1 Hz with an AC perturbation amplitude of 10 mV under open-circuit potential conditions. For photocurrent measurements, the potential was held at 0 V vs. Ag/AgCl, and the working electrode was periodically illuminated with a 365 nm LED light source (98 mW cm^{-2}) in 15 s light on/off cycles.

Text 7. Stability Experiments of Ag-TiO_2.

10 mg of catalyst was dispersed in 20 mL of ultrapure water in the reactor. The system was purged with C_3H_6 gas before illumination. The gas products were analyzed after 3 h. Subsequently, the catalyst was separated by centrifugation, redissolved in 20 mL water, and prepared for the next experiment.

Text 8. Scaling-Up System on Automatic Sunlight Tracking Reactor.

The enlarged experiment was conducted in an outdoor automatic sunlight tracking reactor. The reactor was equipped with a convex lens with an area of 2500 cm^2, focusing sunlight within a 100 cm^2 area. The system included a photosensitive component for automatic solar tracking, ensuring sunlight always struck the convex lens surface perpendicularly. Additionally, the system featured a condensation water circulation device to maintain the reaction temperature at 20 °C. 200 mg of Ag-TiO_2 catalyst was dispersed in 500 mL of deionized water, forming a uniform suspension after ultrasonication, and transferred to a custom-made photocatalytic reactor. Prior to the reaction, the system was vacuumed and purged with C_3H_6 gas for 30 min to eliminate air

completely. The photocatalytic reaction took place between 9:00 and 15:00 daily, utilizing natural sunlight as the light source. Gas and liquid phase products were collected every 30 min during the reaction. The experiment underwent 5 cycles, with each cycle lasting 6 h, and all testing methods aligned with laboratory experiments.

Text S9. The details of EPR experimental

In a typical procedure, 2 mg of the catalyst was dispersed in 4 mL of an aqueous solution containing 100 mM TEMPO. The suspension was thoroughly degassed by vacuum and subsequently purged with Ar gas for 30 min to completely remove oxygen. The reaction system was then irradiated with monochromatic light at 365 nm. Aliquots were taken for analysis after 0 min (dark) and 10 min of illumination to evaluate the changes.

Text S10. Infrared Fourier Transform Spectroscopy (DRIFTS) Measurements.

Utilizing *in-situ* Fourier Transform Infrared Spectroscopy (FTIR) technique, the surface adsorption behavior of the Ag-TiO_2 catalyst was studied. The experiment employed a Fourier Transform Infrared Spectrometer (FTIR, Nicolet iS50, Thermo Fisher Scientific) equipped with a high-temperature diffuse reflection reaction cell and an MCT-A detector for *in-situ* testing. A 50 mg sample of Ag-TiO_2 was placed in the reaction cell, purged with high-purity Ar gas at 200 °C for 30 min to thoroughly remove impurities and surface water adsorption from the catalyst. After cooling the system to room temperature, an adsorption experiment was conducted with a mixture of H_2O/C_3H_6 gas, continuing for 30 min to ensure saturation of surface adsorption. Subsequently, a 365 nm LED light with an intensity was utilized as the light source to drive the photocatalytic reaction. Spectra ranging from 4000 to 1000 cm^{-1} were recorded by averaging 32 scans with a resolution of 4 cm^{-1}. The spectra were converted to Kubelka-Munk units using Omnic software for quantification. A control study with D_2O replacing H_2O was conducted while keeping other experimental conditions constant.

Text S11. Product Adsorption Experiments.

A stepwise adsorption method was employed to investigate the adsorption characteristics of the Ag-TiO_2 catalyst toward reaction products. Specifically, 50 mg of the Ag-TiO_2 catalyst was placed in the *in-situ* reaction cell and purged with high-purity Ar at 200 °C for 30 min. After the system was cooled to room temperature, water vapor was introduced for 30 min to achieve adsorption saturation on the catalyst surface. The infrared spectrum collected under this condition was used as the background. Subsequently, under the same conditions, 1,2-PG was introduced, and the infrared spectrum was recorded after adsorption equilibrium was reached. Finally, using the spectrum of the 1,2-PG-saturated adsorbed surface as the new background, acetaldehyde was introduced for adsorption to examine whether acetaldehyde could still exhibit infrared absorption peaks in the presence of both water and 1,2-PG.

The surface reaction mechanism is further confirmed by stepwise adsorption experiments to gain deeper insight into the reaction mechanism. When H_2O was pre-adsorbed on the catalyst surface, the 1,2-PG signals were completely masked, while acetaldehyde bands appeared at 1720–1770 cm^{-1} (C=O stretching) and 2732 cm^{-1} (formyl C–H). In the dark, the DRIFTS spectra of the Ag-TiO_2/C_3H_6/D_2O system exhibit distinct adsorption features of both D_2O and C_3H_6. The bands at 3089 cm^{-1} (C–H), 2965 cm^{-1} (C–H sp^3), 1650 cm^{-1} (C=C), and 1473–1442 cm^{-1} (CH_2) are attributed to molecularly adsorbed C_3H_6. In the stepwise adsorption experiment of D_2O and 1,2-PG over Ag-TiO_2, the D_2O-adsorbed sample showed characteristic O–D stretching (2452 cm^{-1}) and surface –OD (2736 cm^{-1}) bands. When the D_2O-saturated Ag-TiO_2 surface was used as the background, 1,2-PG displayed distinct absorption peaks at 3360 and 2514 cm^{-1}. Since the characteristic absorption bands of 1,2-PG largely overlap with those of H_2O, making it difficult to distinguish their respective contributions in the H_2O system.

Section 2 Figures

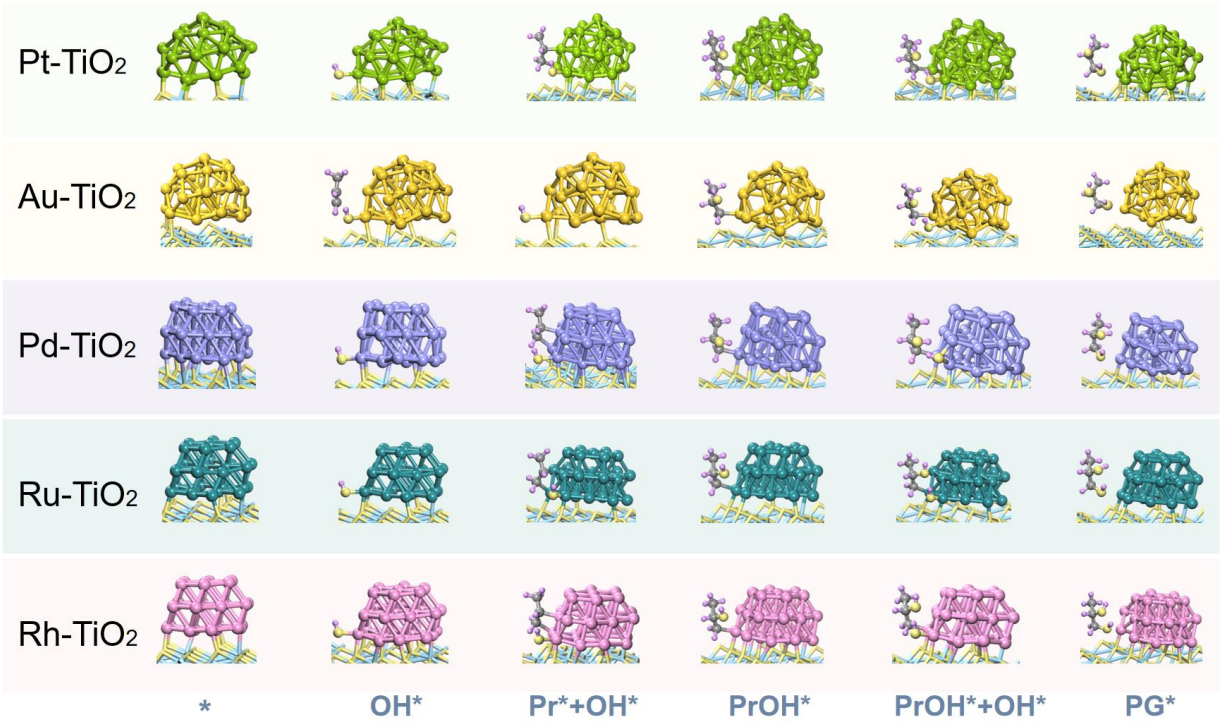


Fig. S1 DFT calculations of the C_3H_6 dihydroxylation reaction on different metal-TiO_2 catalysts using a ball-and-stick model. (color code: gray, C; light yellow, O; light purple)

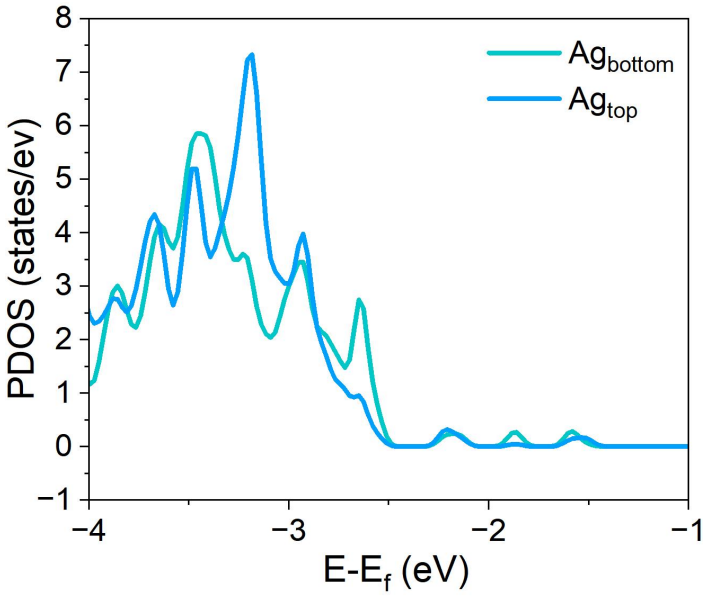


Fig. S2 Projected density of states (PDOS) of the top and bottom regions of Ag nanoparticles in the Ag-TiO_2 catalyst.

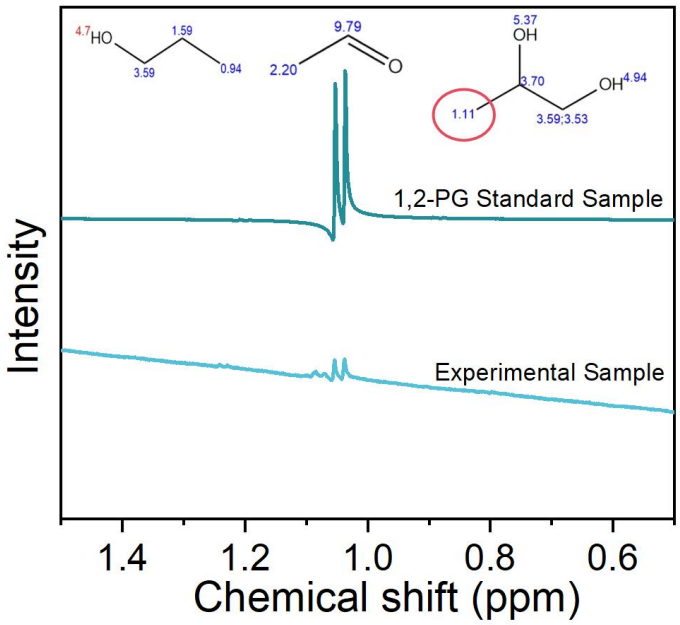


Fig. S3 ^{1}H NMR spectrum of the main product 1,2-PG.

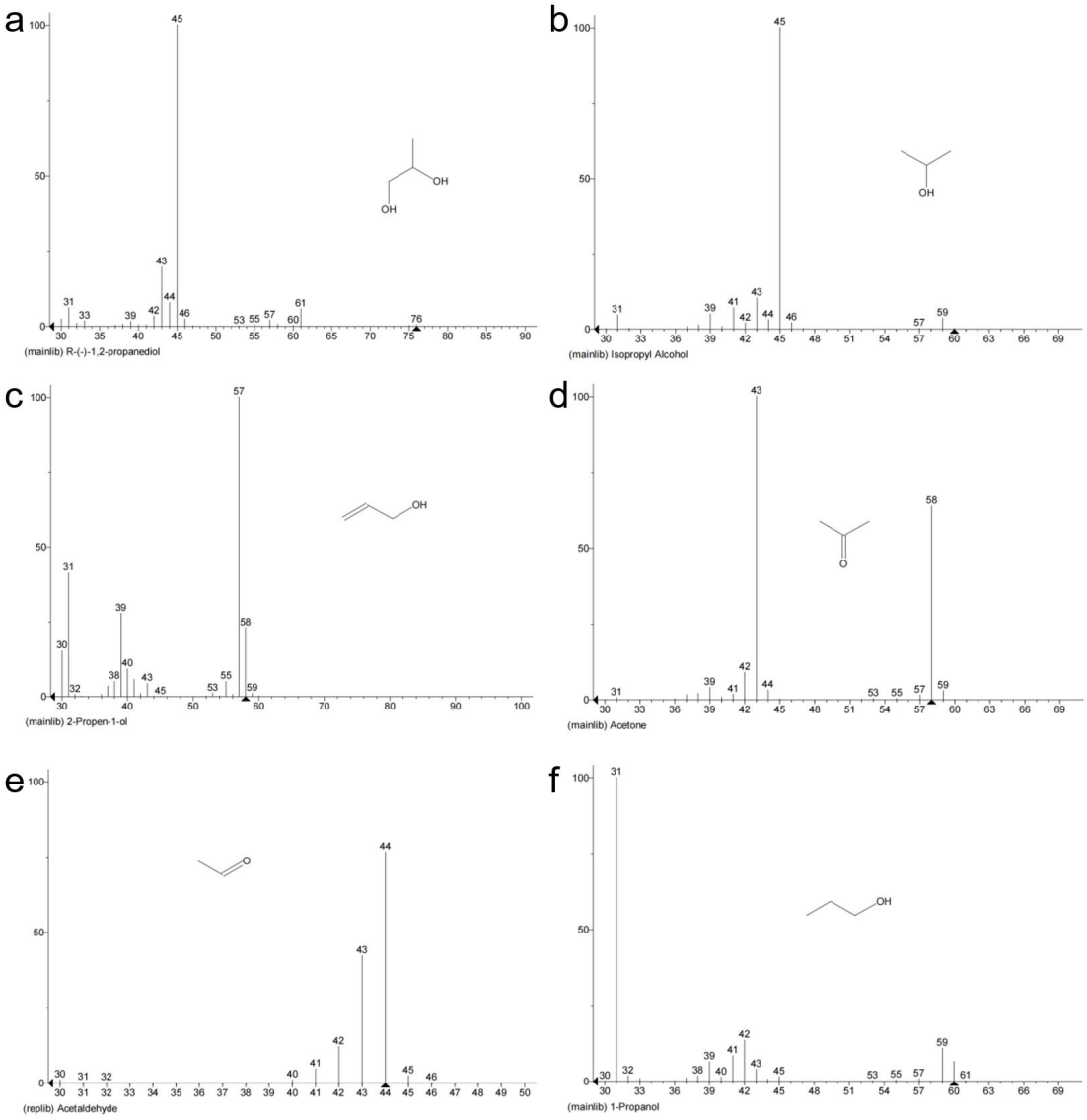


Fig. S4 GC-MS analysis of the reaction products. Several parallel reaction pathways to account for the formation of the main products are given below:

(1) 1,2-PG formation pathway:

$TiO_2 + h\nu \rightarrow h^+ + e^-$

$H_2O + h^+ \rightarrow {}^*OH + H^+$

$H^+ + e^- \rightarrow 0.5H_2$

$^*OH + CH_2{=}CH{-}CH_3 \rightarrow {}^*CH(OH){-}CH_2{-}CH_3$

$^*OH + {}^*CH(OH){-}CH_2{-}CH_3 \rightarrow CH_2(OH){-}CH(OH){-}CH_3$

(2) Allyl alcohol formation pathway:

$H_2O + h^+ \rightarrow {}^*OH + H^+$

$H^+ + e^- \rightarrow 0.5H_2$

$CH_2{=}CH{-}CH_3 + {}^*OH \rightarrow {}^*CH_2{=}CH{-}CH_2 + H_2O$

$^*CH_2{=}CH{-}CH_2 + {}^*OH \rightarrow CH_2{=}CH{-}CH_2OH$

(3) n–Propanol and isopropanol formation pathways:

$H_2O + h^+ \rightarrow *OH + H^+$

$H^+ + e^- \rightarrow *H$

$CH_2{=}CH{-}CH_3 + *OH \rightarrow *CH_2{-}CHOH{-}CH_3$

$*CH_2{-}CHOH{-}CH_3 + *H \rightarrow CH_3{-}CHOH{-}CH_3$

$CH_2{=}CH{-}CH_3 + *OH \rightarrow *CH_2OH{-}CH{-}CH_3$

$*CH_2OH{-}CH{-}CH_3 + *H \rightarrow CH_2OH{-}CH_2{-}CH_3$

(4) Acetaldehyde and CO_2 formation pathways:

$H_2O + h^+ \rightarrow *OH + H^+$

$H^+ + e^- \rightarrow *H$

$CH_2{=}CH{-}CH_3 + *OH \rightarrow *CH_2OH{-}CH{-}CH_3$

$*CH_2OH{-}CH{-}CH_3 + *H \rightarrow CH_2OH{-}CH_2{-}CH_3$

$*CH_2OH{-}CH_2{-}CH_3 + 2*OH \rightarrow CHO{-}CH_2{-}CH_3 + 2H_2O$

$CHO{-}CH_2{-}CH_3 + 2*OH \rightarrow *COOH{-}CH_2{-}CH_3 + H_2O$

$*COOH{-}CH_2{-}CH_3 + *OH \rightarrow *CH_2{-}CH_3 + CO_2 + H_2O$

$*CH_2{-}CH_3 + 13*OH \rightarrow 2CO_2 + 9H_2O$

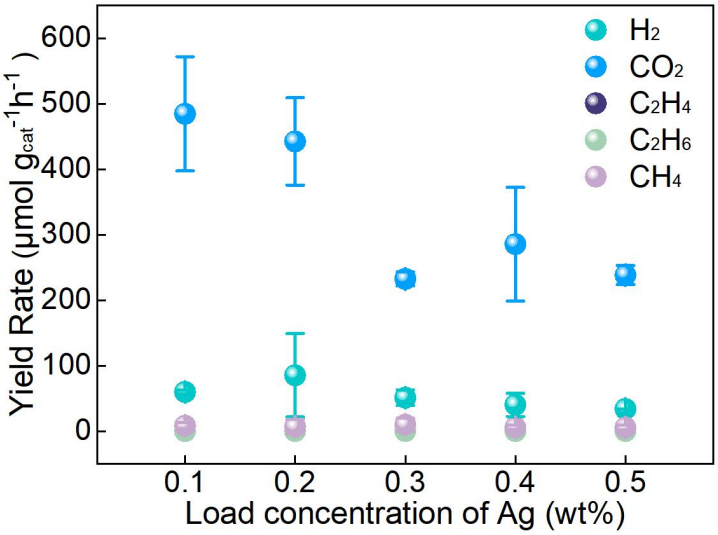


Fig. S5 Comparison of hydrogen evolution rates over Ag-TiO_2 catalysts with different Ag loadings.

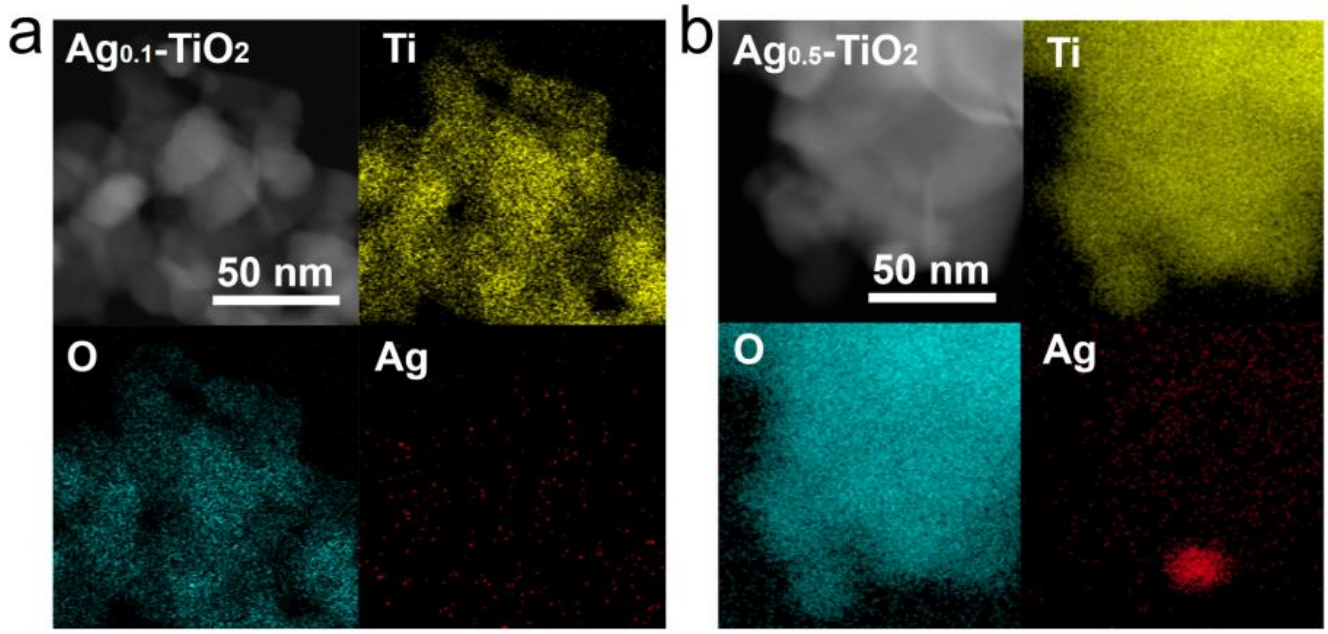


Fig. S6 The corresponding EDS mappings of the Ag-TiO_2 samples with (a) 0.1 wt% and (b) 0.5 wt% Ag loadings.

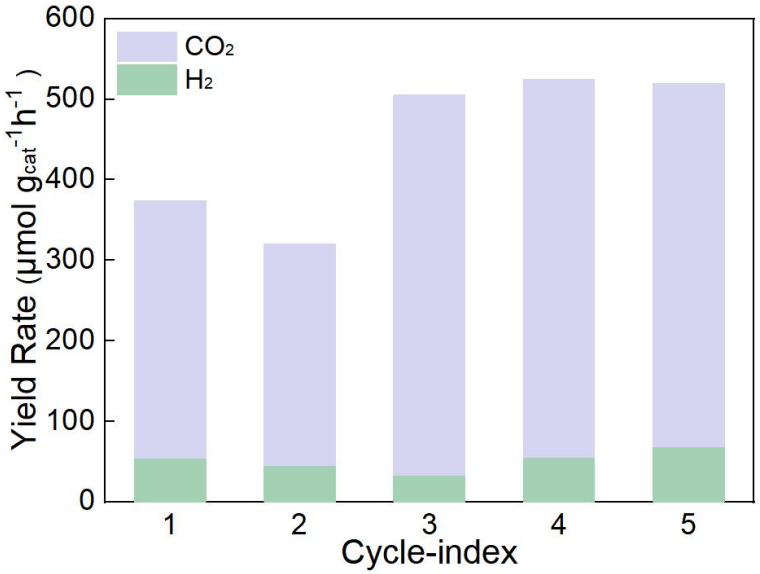


Fig. S7 Gas yields of Ag-TiO_2 during photocatalytic recycling tests.

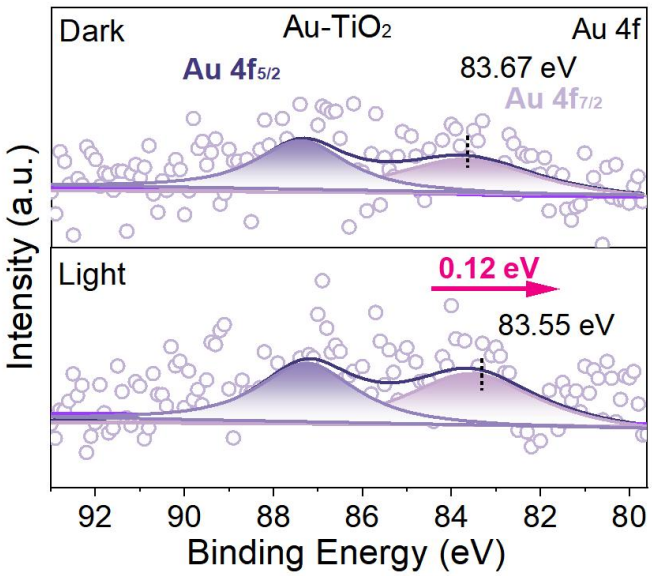


Fig. S8 *In-situ* X-ray photoelectron spectroscopy of Au-TiO_2 (Au 4*f*).

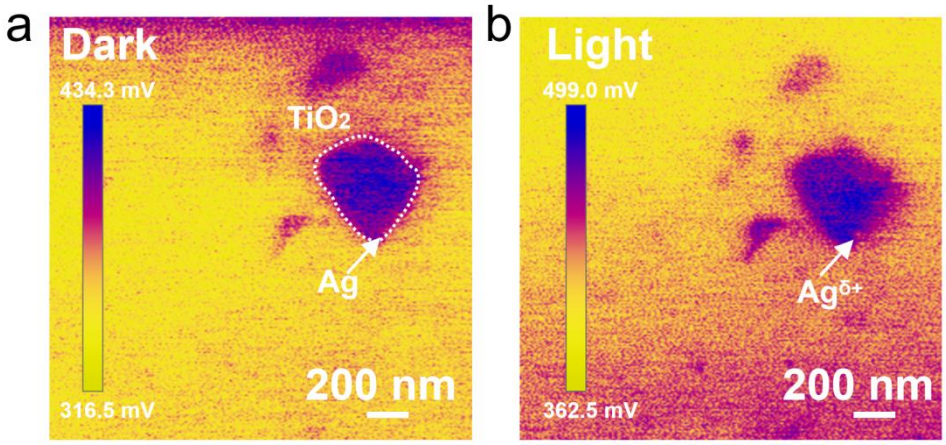


Fig. S9 Surface potential changes of Ag-TiO_2: SPV distributions in the dark (a) and under illumination (b).

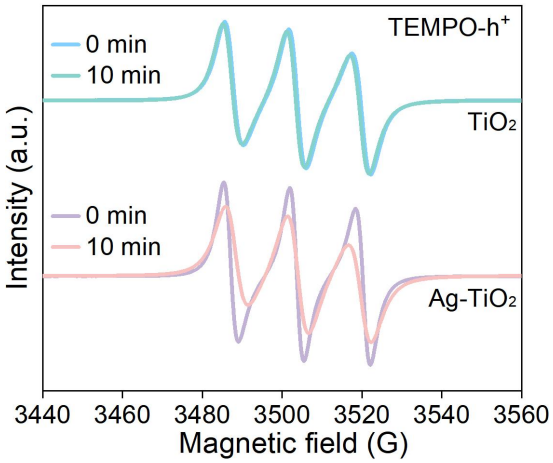


Fig. S10 EPR spectra with TEMPO as the spin-trapping agent

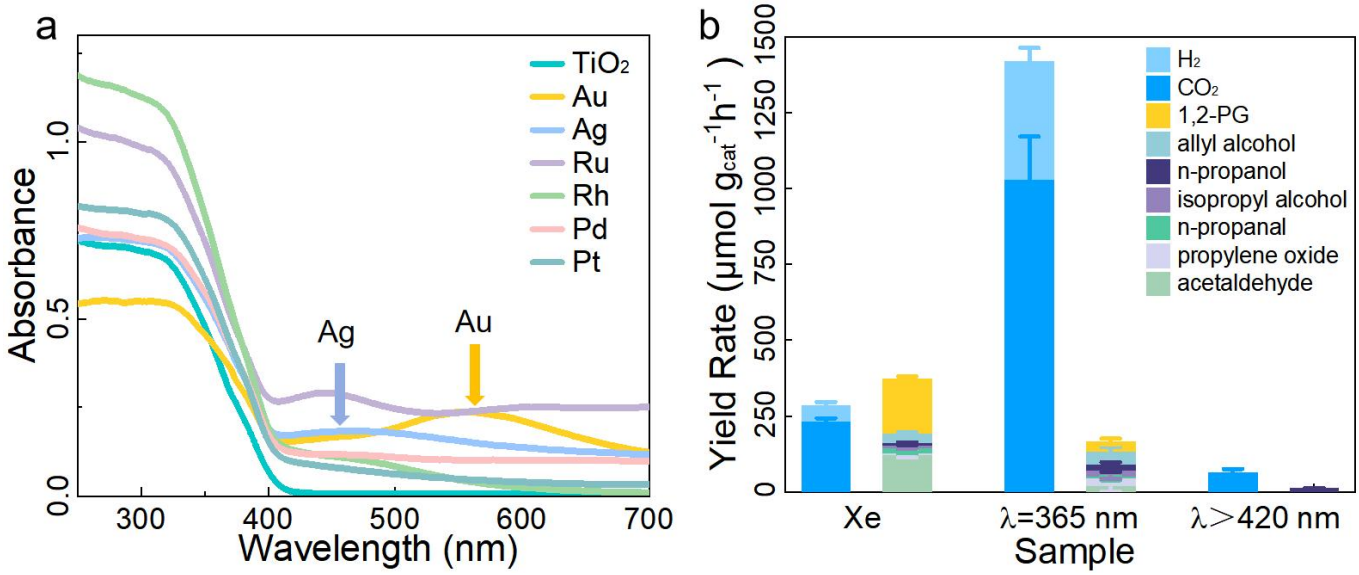


Fig. S11 (a) UV-Vis-NIR DRS of pristine TiO_2 and TiO_2 loaded with different metal nanoparticles. (b) Photocatalytic activity of Ag-TiO_2 under Xe, ultraviolet light, and visible light irradiation ($\lambda > 420$ nm)

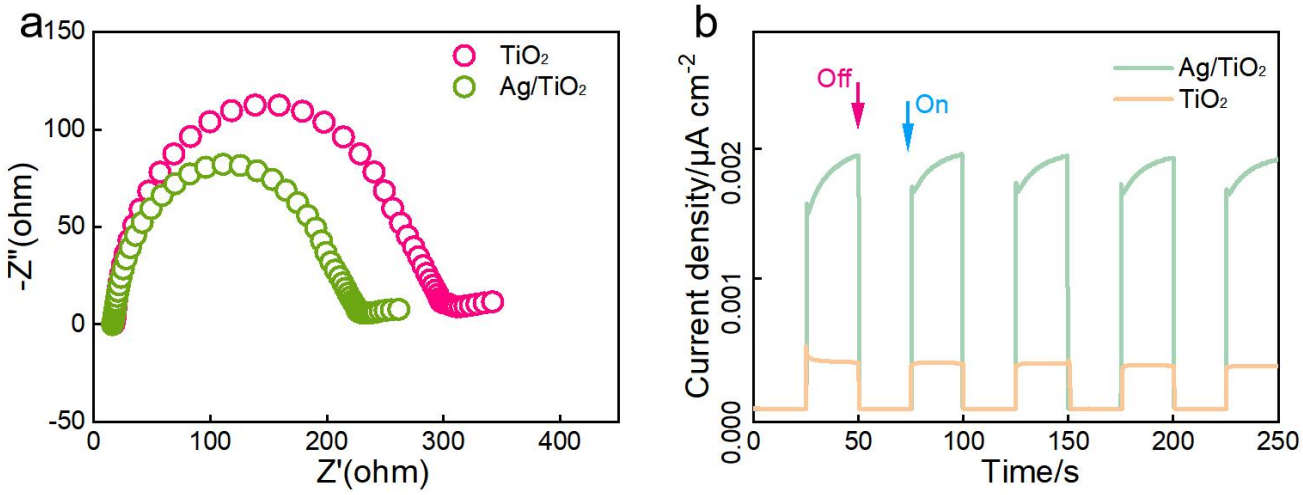


Fig. S12 Comparison of charge transfer and photoresponse behaviors of TiO_2 and Ag-TiO_2 catalysts. (a) Electrochemical impedance spectra (EIS) of TiO_2 and Ag-TiO_2. (b) Transient photocurrent response under light on/off cycles.

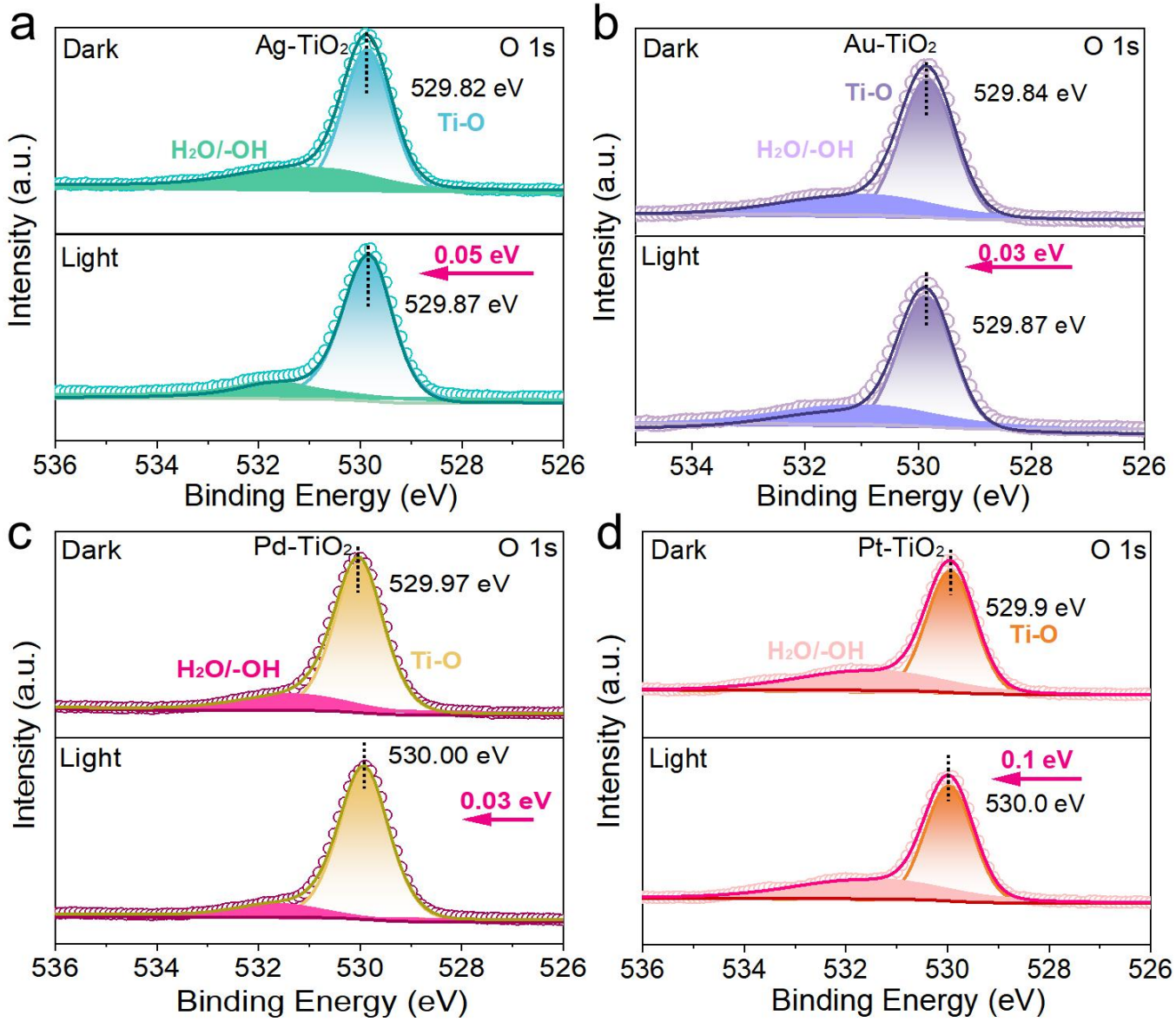


Fig. S13 *In-situ* X-ray O 1*s* photoelectron spectroscopy of a) Ag-TiO_2, and b) Au-TiO_2, c) Pd-TiO_2, d) Pt-TiO_2.

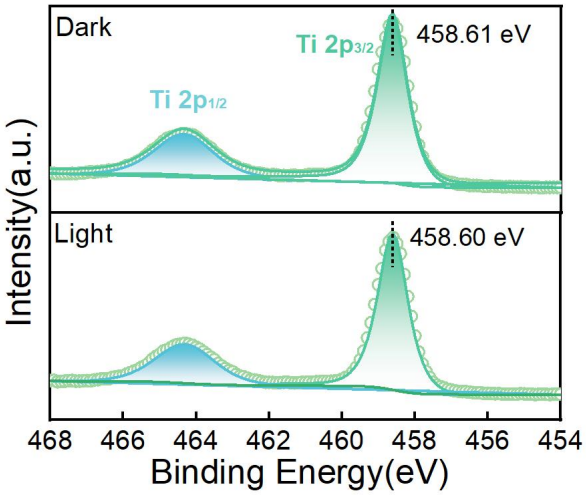


Fig. S14 Ti 2*p* XPS spectrum of Ag-TiO_2

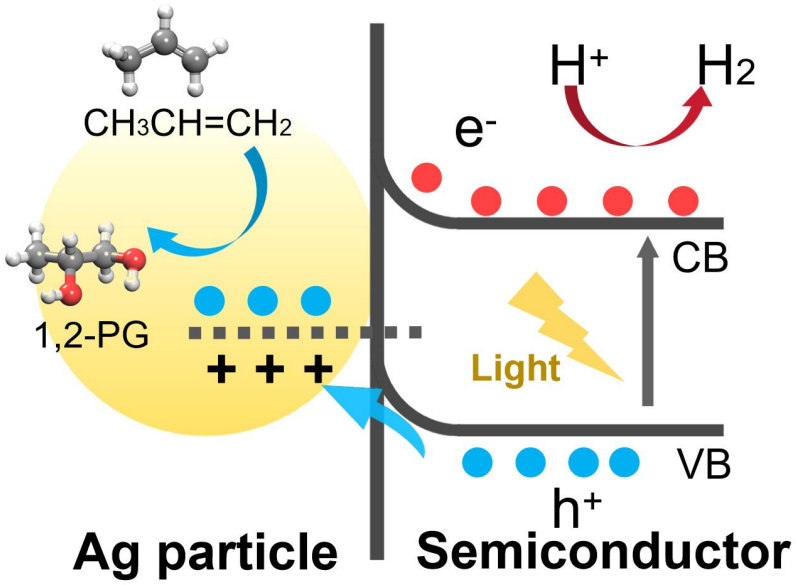


Fig. S15 Photocatalytic mechanism diagram.

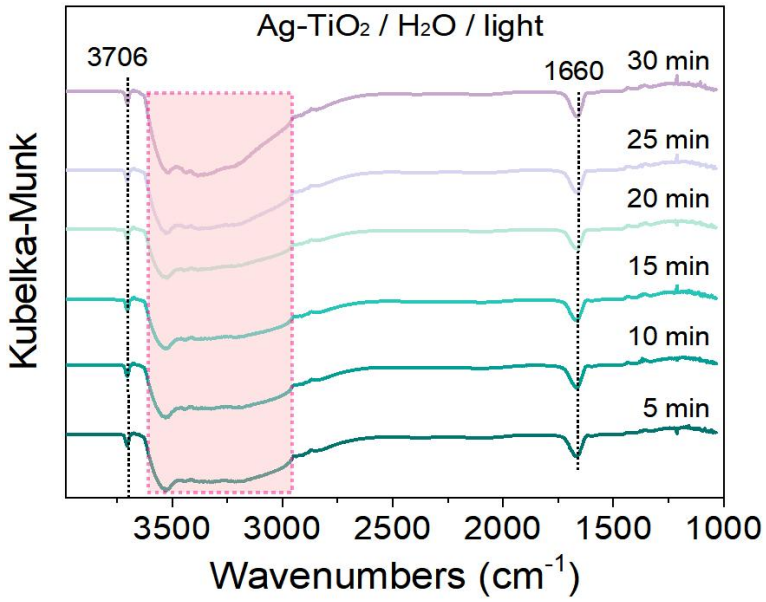


Fig. S16 Time-resolved *in-situ* DRIFTS spectra of Ag-TiO_2 during photocatalytic H_2O activation.

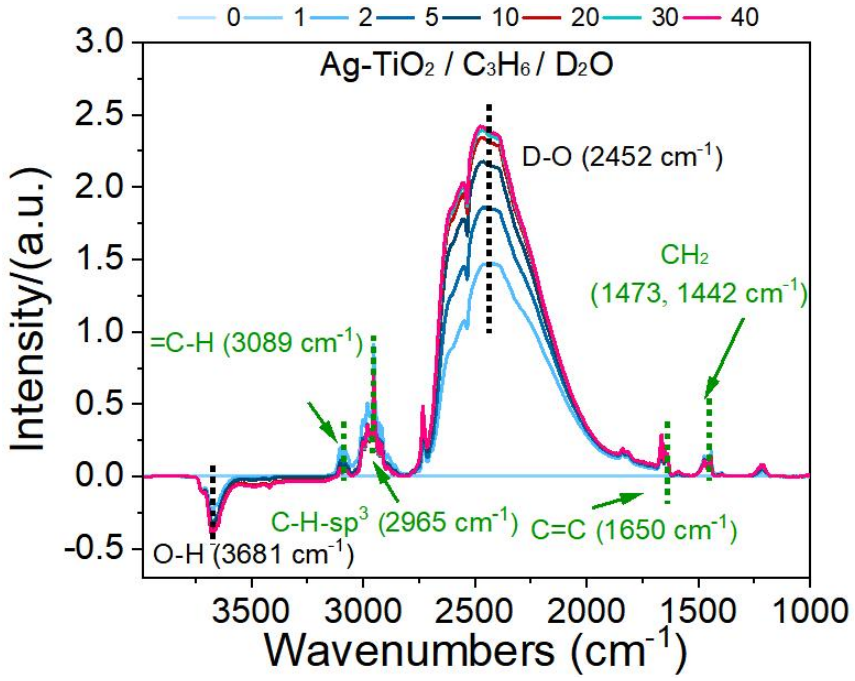


Fig. S17 *In-situ* DRIFTS study of C_3H_6 + D_2O co-adsorption.

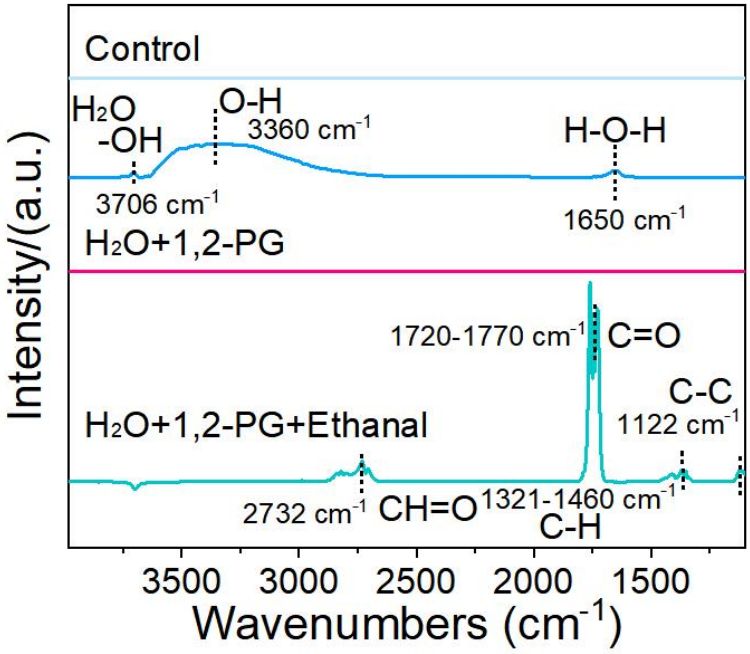


Fig. S18 Infrared adsorption experiment: Stepwise adsorption: H_2O → 1,2-PG → acetaldehyde. The Ag-TiO_2 was first saturated with H_2O vapor, and this state was used as the background for subsequent adsorption of 1,2-PG. Following this, the co-adsorbed state of H_2O and 1,2-PG served as the new background for the final adsorption step of ethanal.

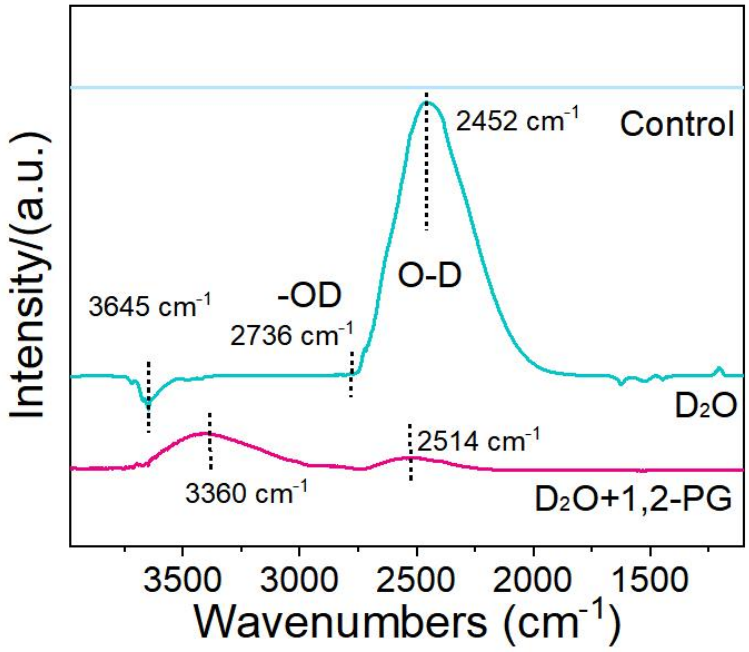


Fig. S19 Isotopic stepwise adsorption with D_2O. The Ag-TiO_2 was first saturated with D_2O vapor, and this state was used as the background for subsequent adsorption of 1,2-PG.

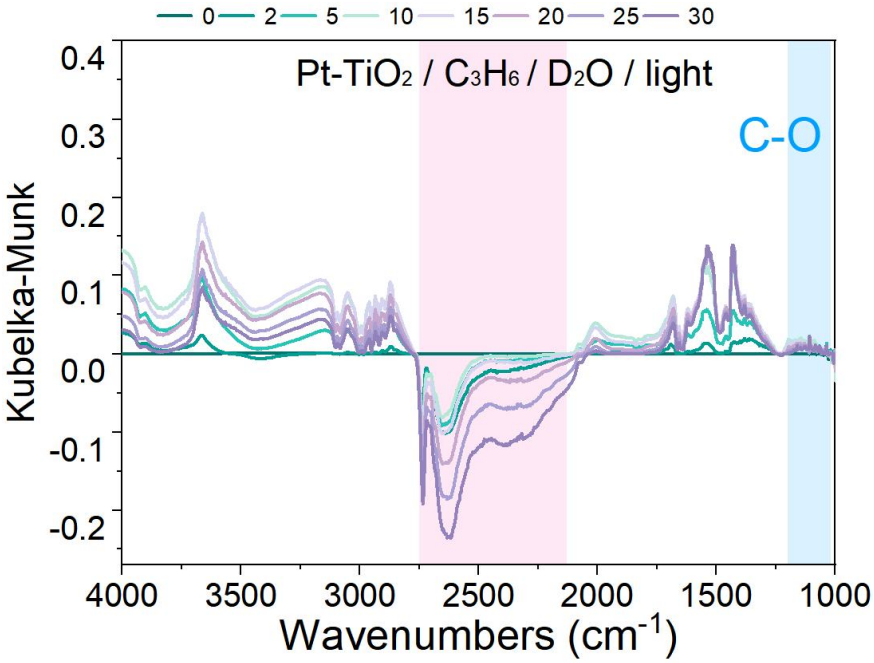


Fig. S20 *In-situ* DRIFTS spectra of photocatalytic reactions using D_2O instead of H_2O of Pt-TiO_2 from 0 min to 30 min.

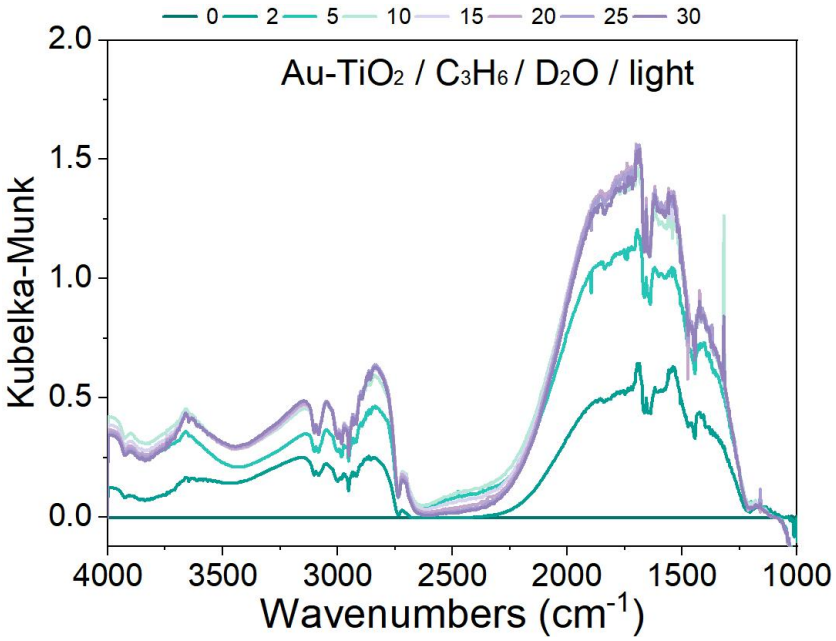


Fig. S21 *In-situ* DRIFTS spectra of photocatalytic reactions using D_2O instead of H_2O of Au-TiO_2 from 0 min to 30 min.

Reference

[S1] J. Jen, M. Leu, T. Yang, *J. Chromatogr. A,* **1998**, 796, 283–288.